

A new survey of diffuse interstellar bands (5650 – 6865 Å)^{*}

T. Weselak¹, M. Schmidt², and J. Kręłowski¹

¹ Nicolaus Copernicus University, Center for Astronomy, Gagarina 11, Pl-87-100 Toruń, Poland
e-mail: tomcat@astri.uni.torun.pl, jacek@astri.uni.torun.pl

² Nicolaus Copernicus Astronomical Center, Rabiańska 8, Pl-87-100 Toruń, Poland
e-mail: schmidt@ncac.torun.pl

Received December 17, 1998; accepted November 10, 1999

Abstract. This paper presents a new systematic survey of diffuse interstellar bands in the optical wavelength range from 5650 to 6865 Å based on echelle spectra of medium-reddened early-type stars acquired at McDonald Observatory. Adding up interstellar spectra of the same type (as it was done by Kręłowski et al. 1997) we reached a very high signal-to-noise ratio. In this spectral range 89 new features have been discovered, 62 of them certain. In the whole spectral range of this survey we have found 240 features, 213 of them certain.

Key words: ISM: general — ISM: molecules

1. Introduction

The “stationary” spectral features at 5780 Å and 5797 Å, observed by Heger (1922) at the Lick Observatory are the first discovered members of the set of Diffuse Interstellar Bands (DIBs). The interstellar origin of several strong DIBs has been proven by Merrill (1934), Beals & Blanchet (1937), York (1971) and Herbig (1975). The latter work based on photographic spectra of the S/N ratio enhanced by means of averaging, pointed the possible existence of weak 5784 and 5795 (near 5797) bands. These weak DIBs as well as some other similar features may be related to some of the strong ones as pointed by Chlewicki et al. (1987) and are more evident in “zeta” targets – i.e. those in which the strength ratio of 5797 and 5780 is relatively high (Kręłowski & Westerlund 1988). During recent years the number of known DIBs keeps growing. The paper of Smith et al. (1981) suggested that the feature near 6194.5 Å is a very weak DIB, well seen in spectra of dark interstellar

clouds. Generally many very weak features were successfully detected by Ferlet et al. (1983), Herbig (1988) and by Herbig & Leka (1991) in the red and near infrared spectral ranges.

The survey of Kręłowski & Sneden (1993) proved the existence of very weak DIBs in the vicinity of the 5780 and 5797 bands and shortward of the 6196 band. Last surveys of Kręłowski et al. (1995) and Kręłowski et al. (1997) proved that number of very weak features grows with resolution and signal-to-noise ratio. The most complete survey (Jenniskens & Désert 1994) covered a broad spectral range from ~3800 to ~8700 Å in the spectra of heavily reddened, early type stars. Based on a very small sample (only four stars) this survey detected hundreds of weak features, some of them not known in previous works, but the resolution and signal-to-noise ratio were not high enough to discover very weak DIBs. Also the small sample has not allowed to investigate the behaviour of the weak vs. strong DIBs in different environments.

The presented survey is based on high quality spectra of moderately reddened early spectral type stars. The method of averaging spectra to get a very high signal-to-noise (Kręłowski et al. 1997) makes possible to detect very weak, shallow features never known before. Results of this survey confirm the existence of the already discovered features; additionally many new very weak ones were discovered. These are presented both in tabulated form and as the set of plots showing the spectra in the whole range of this survey.

2. Observations

The observations have been made by one of us (JK) at the McDonald Observatory in Texas during 1993 using the Cassegrain echelle spectrograph fed with the 2.1-m telescope. A typical spectrum is divided into 26 orders covering the range from ~ 5600 to ~ 7000 Å (one order consists

^{*} Figure 4 is only available in electronic form at <http://www.edpsciences.org>

of 1200 pixels in the wavelength scale). The instrument described by McCarthy et al. (1993) consists of refractive collimator and camera optics, a 23.2 ℓ/mm echelle grating with a blaze angle of 65° , a prism cross-disperser and a Reticon 400×1200 CCD with $27 \times 27 \mu\text{m}$ pixels. This configuration gives the effective resolution $R = 64\,000$ and spectral dispersion of $0.050 \text{ \AA}/\text{pixel}$ at 5790 \AA . The S/N ratio for spectra of individual stars is typically ~ 500 but is not constant inside a spectrum, even inside one order. Some of the features are easier to detect while situated in a “better” segment of an investigated spectrum. To obtain high S/N for the final spectra of individual stars the multiple exposures of many program stars were obtained. This signal-to-noise ratio in any spectrum of an individual object is not high enough for detection of very weak features and thus the method of improvement the signal-to-noise is desirable. The detailed methods of data reduction for obtaining spectra of individual stars are described by Krelowski & Sneden (1993). Out of the ~ 80 objects observed at McDonald Observatory during 1993 we selected 14 targets listed in Table 1.

Spectrum of each selected star is characterized by a very narrow and symmetric absorption lines D_1 and D_2 of the interstellar sodium. The widths in Å of interstellar sodium lines measured on the level of half continuum for our program stars are presented in Table 1. These features allow us to shift the wavelength scale of the spectra to the rest wavelength scale for interstellar clouds, and thus to determine the rest wavelengths of the observed DIBs (the last column of Table 1 presents shifts in pixels for interstellar sodium lines in spectra of our stars). Narrow and symmetrical profiles of sodium lines allow us to suppose that our targets are probably obscured by single clouds (see widths of Na D lines in spectra of our program stars listed in Table 1 in Cols. ΔD_1 and ΔD_2). It is obvious that towards our targets, except HD 210839 we do not observe any detectable Doppler splitting. Thus the latter cannot be expected inside DIB profiles which are broader. Additionally the chosen targets are fast rotators and thus a spectrum of each star is free of weak stellar features containing only strong ones as well as interstellar features and telluric lines.

Figure 1 shows the spectra of a program star (HD 23180) and the divisor (Spica) before division and the resultant spectrum after the cancellation of atmospheric features in the Na D spectral region (thick line). To cancel the telluric lines the spectrum of each star was divided by divisor spectrum (Spica in most of cases) in the whole range of this survey.

The selected objects belong to two distinct types coded as “sigma” and “zeta” in accordance to the strength ratio of the central depths of the two strong DIBs: 5780 and 5797 (see 5780/5797 column in the Table 1). All our targets rotate with high velocities. The only one star with smaller rotational velocity listed in Table 1 (HD 23180) is a typical “zeta” type target. Observational material

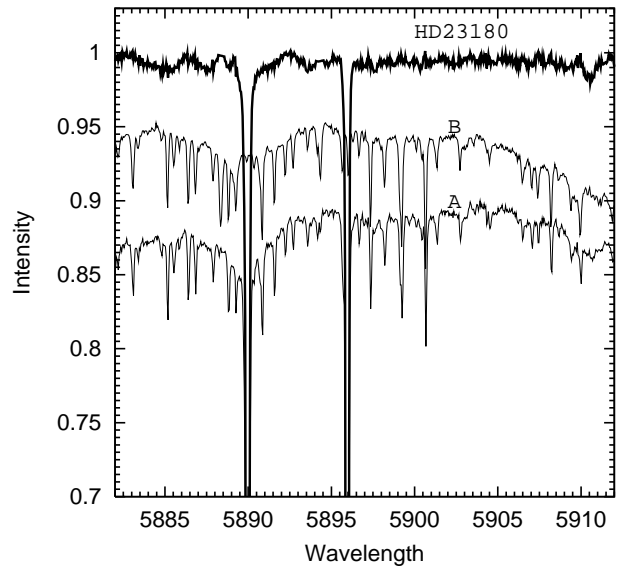


Fig. 1. The cancellation of H_2O contamination in the region of interstellar sodium Na D lines in the spectrum of HD 23180. The lowest (A) spectrum was divided by Spica spectrum (B). The spectrum of the HD 23180 at the top of the panel contains no telluric lines only interstellar features (clearly seen DIB at 5910.40 \AA)

allows us to select only a couple of each cloud type. These samples can hardly be much extended as a great majority of bright OB stars is observed through several interstellar clouds each. The merging procedure is the averaging of the overlapping wavelength ranges of two neighbour echelle orders. The points are weighted – the weight is proportional to the distance from the edge where the S/N is lowest. Before the merging procedure (described by Krelowski & Sneden 1993) the telluric line removal has been accomplished. This procedure and continuum placement at the ends of echelle orders is somewhat arbitrary at the $\pm 1\%$ level. This uncertainty does not affect the detection of very weak features which are typically “narrow”, but it compromises the ability to detect the broad and shallow features which stretch over more than one echelle order. As the arbitrarily chosen continuum level in the case of spectra of individual stars (used for achieving spectra of “sigma” or “zeta” clouds) makes measurements of weak features difficult (see Krelowski & Sneden 1993) we measured equivalent widths of new features in the spectrum of HD 210839.

3. Searching for new DIBs

3.1. Average spectra

Since the publication of Krelowski & Walker (1987) it is clear that the strong diffuse bands at 5780 and 5797 Å are not of the same origin. Their strength ratio varies from object to object. In Table 1 we present 9 targets in which the 5780/5797 strength ratios resemble

Table 1. Basic stellar data

HD	Name	Sp/L	V	$E(B - V)$	$v \sin i$ km s ⁻¹	cloud type	5780/5797	ΔD_1 Å	ΔD_2 Å	shift pixels
23180	o Per	B1 III	3.82	0.26	85	ζ	0.6	0.18	0.15	-16
24912	ξ Per	O7.5 III	4.02	0.29	216	σ	1.7	0.28	0.23	-14
141637		B3 V	4.64	0.16	300	σ	2.5	0.26	0.20	+7
142096		B2 V	5.03	0.20	197	σ	3.0	0.17	0.11	+7
142114		B2 V	4.59	0.14	308	σ	2.5	0.17	0.11	+9
142184		B2 Vne	5.42	0.16	349	σ	1.6	0.32	0.30	+9
144217	β^1 Sco	B0.5 V	2.62	0.17	130	σ	2.7	0.15	0.12	+7
144470	ω^1 Sco	B1 V	3.96	0.19	142	σ	1.8	0.18	0.17	+7
145502	ν^1 Sco	B3 V	4.01	0.25	199	σ	1.9	0.20	0.15	+7
148184		B2 IVpe	4.42	0.49	134	ζ	0.9	0.28	0.17	+8
149757	ζ Oph	O9.5 V	2.56	0.29	379	ζ	0.8	0.21	0.19	+11
179406		B3 V	5.34	0.32	150	ζ	0.7	0.32	0.30	+15
184915	κ Aql	B0.5 III	4.95	0.22	259	σ	1.9	0.25	0.19	+15
*210839		O6Iab:	5.06	0.52	285	σ/ζ	1.0	0.75	0.73	+1

that of HD 147165 (σ Sco) and 4 targets similar to HD 149757 (ζ Oph). These two types of objects can be classified as “sigma” and “zeta” type clouds (Krelowski & Sneden 1995). The calculated average of $\lambda 5780$ and $\lambda 5797$ strength ratio is 2.2 for the “sigma” cloud and 0.75 for “zeta” type cloud. Our observational material involves only bright stars; such objects can be considered as nearby and thus very likely to be seen through single, individual clouds (“sigma” or “zeta” type). Adding up separately “sigma” and “zeta” type spectra we reach a very high signal-to-noise ratio, characteristic for two types of interstellar clouds (see Krelowski et al. 1997).

Figure 2a presents the spectral region in the vicinity of $\lambda 5780$ for four “zeta” type stars, which were used in procedure of adding up spectra. The weak features shortward of $\lambda 5780$ are clearly seen in all four targets. The spectra seen in Fig. 2a were used to obtain average “zeta” type spectrum, seen on the top of Fig. 2b. At the bottom of this figure we present the spectrum of HD 179406 and the next spectra to the top show the effect of adding up spectra of stars shown in Fig. 2a with the average zeta type spectrum seen at the top of this figure. The average spectra of “sigma” and “zeta” type are of very high signal-to-noise ratio (see the measured values of S/N in the vicinity $\lambda 5762.69$ in Fig. 2b), which is very important for detection of weak interstellar features.

Figure 3a shows the spectral region of weak atomic doublet of interstellar Lithium at 6707.9 Å seen in three spectra of “zeta” type clouds. The spectrum of HD 23180 as of poorer quality in this spectral range was not included. In Fig. 3b we present the effect of adding up the spectra

seen in Fig. 3a. In the vicinity of Li I line are seen three weak DIBs and one unidentified stellar line marked with the sign # (see Sect. 3.2). Interstellar Li I line seen only in several targets is too weak to be observed in most of individual targets and could not be used for shifting the wavelength scale of the spectra to the rest wavelength of these lines. The line is not detectable in any of our “sigma” targets – only in the average spectrum (see Fig. 4).

The most heavily reddened star in Table 1, HD 210839, is a special target which is used to verify presence of weak interstellar features. This star was observed twice during one observational session at McDonald Observatory and these two spectra were averaged giving as a result a very high signal-to-noise ratio. It is also one of the most rapidly rotating targets which spectrum (O6) should contain only a few, broad lines and thus all observed narrow features (after the removal of telluric lines) are to be considered as interstellar.

3.2. Stellar lines

As an additional check of the interstellar origin of observed features, we have made identification of stellar lines in the available spectral range. To this purpose we have synthesized a number of spectra with temperatures characteristic for the observed spectral types and gravities. All calculations have been made with Hubeny’s SYNSPEC code (Hubeny et al. 1986; Hubeny et al. 1995). As input atmospheric models we applied Kurucz’s grid (Kurucz 1992) using the list of lines from Kurucz’s CD ROM

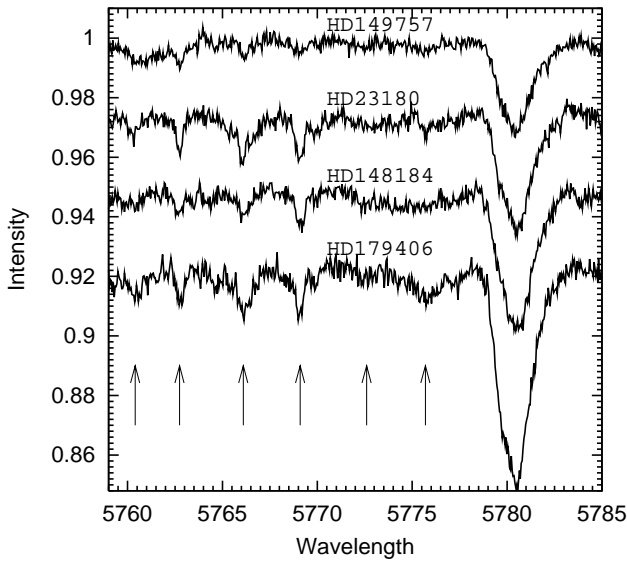


Fig. 2. a) The spectra of four zeta type stars in the region of weak features shortward of $\lambda 5780$

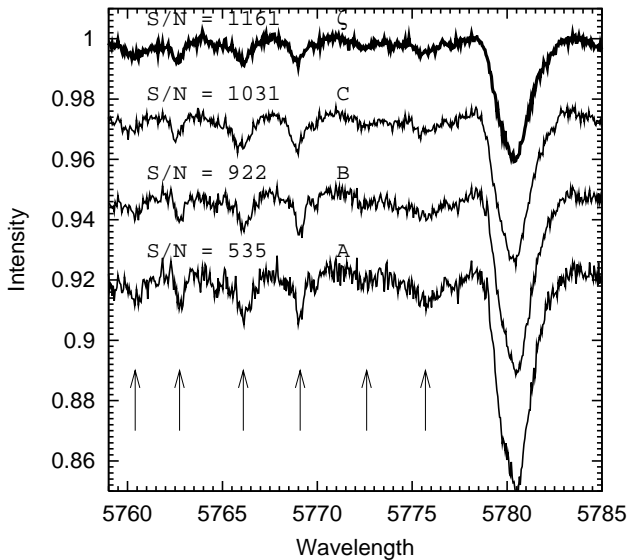


Fig. 2. b) The effect of adding up the spectra seen in Fig. 2a. A—the spectrum of star HD 179406. Spectrum B corresponds to the sum of spectra HD 179406 and HD 148184 added up and normalized to unity. C involves the spectrum originating from the three bottom spectra seen in Fig. 2a. D—all considered spectra summarized. In each case we present measured S/N in the vicinity $\lambda 5762.69$

No. 23 (Kurucz 1990) and occasionally the VALD database mailserver (Piskunov et al. 1995). The procedure of dividing the spectra under consideration by the spectra of rapidly rotating standards and averaging of the stellar spectra of slightly different types and different radial velocities transforms the shapes of stellar features and leaves some complex structures in the resulting spectra. In such places the search for weak

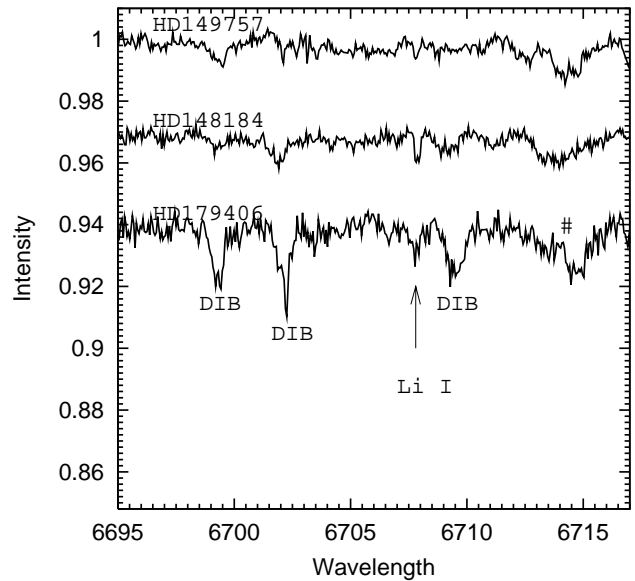


Fig. 3. a) Interstellar Li I line at 6707.9 \AA seen in three program stars (spectrum of HD 23180 is not included as it has smaller S/N in this spectral range)

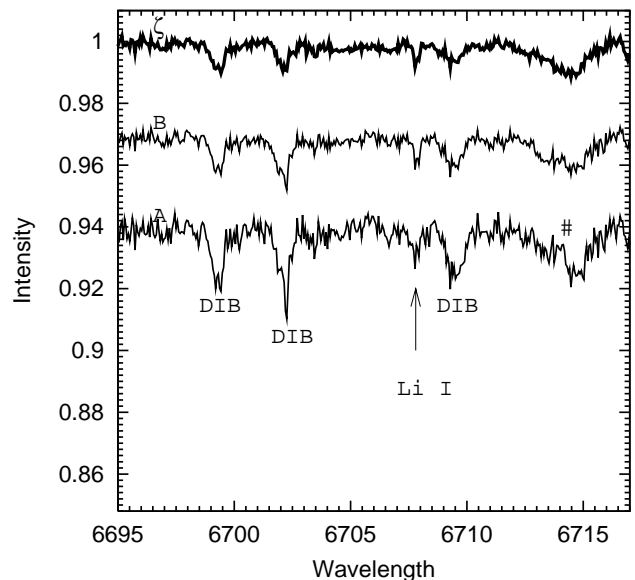


Fig. 3. b) The effect of adding up the spectra seen in Fig. 4. A—the spectrum of star HD 179406. Spectrum B corresponds to the sum of spectra HD 179406 and HD 148184 added up and normalized to unity. C—all considered spectra summarized (“zeta” type spectrum)

interstellar features is very difficult. Having this in mind we have identified the stellar lines being source of these features. Some features seen in the averaged spectrum of “zeta” type originate in the binary object (o Per?) and their shapes are more complicated than one expects from the synthesized spectrum. At last, there are four features of stellar origin which remain unidentified. Both of them have been marked with the sign # in Fig. 4.

Table 2. List of certain DIBs. Codes: br: broad, bl: blended with stellar and/or telluric lines, a: very strong, b: strong, c: quite strong, d: weak, e: very weak, f: not detectable

λ_{lab} Å	$EW \star$ mÅ	In σ cl.	In ζ cl.	references
5705.43:	25.4	c, br	d, br	H75 J94
5719.40	5.8	d	d	J94
5756.07		f	e	K97
5760.44	1.0:	e	d	K93 K95 K97
5762.69	3.0	e	d	K93 J94 K95
5766.15	8.4	d	d	Ch87 K93 K95
5769.03	0.5:	e	d	K93 K95 K97
5772.53	7.6	d	d	K93 J94 K95
5775.75	2.1:	d	d	K93 J94 K95
5780.50	245.2	a	a	H75 Ch87 K95
5785.11	2.1:	e	e	K97
5788.90	2.2:	f	e	K97
5793.19	7.6	e	d	K93 K95 K97
5795.20		d, br	d, br	K93 K95 K97
5796.97	bl	b	a	H75 Ch87 K93
5809.22	bl	e	d	K93 J94 K95
5811.57	bl	e	e	K97
5814.21	bl	e	d	K97
5815.78	bl	f	d	K97
5818.69	1.8:	f	d	K93 K95 K97
5821.22	1.7:	f	e	K97
5828.52	4.1	e	d	K93 K95 K97
5830.77	0.5:	f	e	K97
5832.88		f	e	K97
5835.00		f	e	K97
5837.26	0.8:	f	e	K97
5838.08	1.3:	e	d	K97
5840.72	4.4	e	d	K97
5842.49		e	d	K97
5843.42	2.5	d	d	K97
5844.15:		c, br	d, br	H75 H91 J94
5844.80	3.6	d	e	K97
5845.67		e	e	K97
5848.37	0.5:	e	e	new
5849.85	29.0	c	b	H75 Ch87 H91
5852.14	0.4:	e	e	K97
5854.54	1.9	e	d	K97
5855.72	0.7:	e	d	K97
5857.19		e	d	K97
5859.00	0.5:	e	e	new
5860.27	1.4:	e	e	K97
5861.89	1.2:	f	e	K97
5866.50	2.3	d	e	K97
5870.71	bl	d	d	new
5900.56	6.5	e	d	K95
5904.52	0.6:	e	d	K95
5908.33	0.6:	f	e	K95
5910.40	9.5	d	c	K95
5917.51	1.2:	e	e	K95
5922.31	1.8:	e	e	K95
5923.39	8.4	d	d	K95
5925.85	4.5	f	e	K95
5927.70	0.5:	e	d	K95
5928.96	1.2:	e	e	K95
5930.00	bl	f	d	K95
5932.84	1.0:	e	d	new
5942.30	2.8	e	d	new
5945.44	1.4:	e	d	K95
5947.25	6.4	e	d	K95
5948.88	1.4:	e	d	K95
5958.89	15.3:	e	d	new
5965.28	1.3:	e	e	new
5966.28	2.1	e	d	new
5967.63	2.0	d	d	new
5969.88	1.8:	e	e	new
5973.78	2.1	e	d	new
5975.58	2.6	f	d	K95
5982.83	10.4	e	d	H75 K95
5985.38	1.4:	f	e	new
5986.43	2.6	d	e	K95
5988.03	5.7	d	d	K95
5989.48	4.2	f	d	K95
5994.58	1.0:	e	e	new
5995.73	4.6	d	d	K95
5997.58	1.2:	e	e	new
5999.18	2.4	e	e	new
6004.93	10.8	e	e	H91 K95
6010.80:	14.1	e, br	e, br	H75 J94 K95
6017.53	0.5:	d	d	new
6019.23	2.6	d	d	J94 K95
6022.98	1.2:	f	e	K95
6023.88	1.7:	f	e	K95
6027.48	9.4	d	d	K95
6037.38	0.5:	d	d	J94 K95
6057.58	1.0:	e	d	new
6059.28:	3.2	e	f	J94
6060.10:	1.7:	e	e	J94
6065.23	8.2	d	e	J94
6068.23		e	e	new
6070.98:	1.7:	e	d	J94
6082.18	1.0:	f	e	new
6084.78	1.0:	e	d	new
6089.78	12.6	c	c	H91 J94
6093.18	0.9:	e	d	new
6098.53	1.4:	e	d	new
6102.33	1.6:	d	d	new
6108.13	5.9	d	d	K93 J94
6109.98	1.0:	e	d	K93
6113.18	14.9	d	d	H75 H91 K93
6116.83	3.4	e	d	K93 J94
6118.63	1.0:	e	d	K93
6140.03	6.3	d	d	K93 J94
6145.50	4.1	f	d	K93
6158.53		d	d	new
6161.96	4.8	d	d	K93

Table 2. continued

λ_{lab} Å	$EW \star$ mÅ	In σ cl.	In ζ cl.	references	λ_{lab} Å	$EW \star$ mÅ	In σ cl.	In ζ cl.	references
6181.25	0.8:	e	d	new	6497.82	3.0	e	d	J94
6182.60	0.9:	e	d	new	6501.23	2.5	e	d	new
6185.98	2.7	e	d	new	6513.38	1.3:	e	d	new
6187.58	2.1	e	d	new	6516.64	4.6	e	d	new
6189.47	0.5:	e	d	J94	6518.76		e	e	new
6193.06	0.9:	e	d	new	6523.36	1.0:	e	d	new
6194.77	6.9	d	d	S81 Ch87 K93	6536.89	4.3	e	e	new
				J94 K95	6627.88	1.0:	e	f	new
6196.05	34.2	c	c	H75 H91 K93	6660.70	2.5	e	e	new
				J94	6660.70	3.5	e	e	new
6196.96	1.2:	e	d	new	6672.39	1.7:	e	d	K95
6199.04:	1.8:	f	e	new	6518.76	10.0	d	d	J94
6203.05	62.3	c	c	H75 Ch87 H91	6534.14	5.6	e	d	new
				J94	6536.89	0.8:	d	d	J94
6204.86	bl	e, br	d, br	J94	6546.15	3.8	f	d	new
6211.73	2.4	e	d	K95	6548.93	5.2	d	e	new
6212.87	2.1	d	d	K95	6553.89	6.6	d	d	new
6220.77	1.4:	e	d	K95	...				
6223.63	2.5	d	d	K95	6597.34	13.3	d	d	H75 H91
6226.08:	1.3:	e	d	K95	6613.52	148.4	b	a	H75 H91 J94
6234.05	7.4	d	d	H75 J94 K95	6622.90	3.6	d	d	K95
6245.47	5.0	e	d	K95	6627.88	3.1	e	e	new
6250.83	2.4	d	d	new	6632.65	3.4	d	e	J94 K95
6289.86	73.8	c	b	H75 H91	6635.44	4.3	d	e	K95
6283.80	204.4:	a	a	H75 H91 J94	6660.70	31.2	d	c	H75 H91 J94
6287.54	8.4:	f	d	J94	6665.15	3.9	e	d	new
6289.30	1.0:	e	d	J94	6672.39:	9.0	d	d	new
6350.70	4.4	e	d	new	6694.50	5.4	f	e	K95
6353.25	2.9	f	d	H91 J94 K95	6697.01	1.5:	f	e	K95
6358.35	1.7:	f	d	H91 J94	6699.24	18.1	d	d	H75 F83 H91
6362.50	4.4	e	e	H91 J94 K95					J94 K95
6364.44	0.5:	e	d	H84 J94 K95	6701.95	11.0	d	d	F83 H91 K95
6367.41	6.7	e	d	H84 J94 K95	6709.44	0.9:	d	d	K95
6376.10	16.1	d	c	H75 H91 J94	6729.28	2.7	e	d	new
				K95	6737.14	1.8:	e	d	new
6379.46:	53.6	c	b	H75 H91 J94	6740.96	2.6	d	d	J94
6387.18		e	d	new	6767.58	0.9:	d	d	H88
...					6770.12	4.5	e	d	H88 J94
6396.63	bl	e	d	H91 K95	6779.04	4.0	d	e	H88
6400.25	2.7	e	d	K95	6788.66	2.3	e	d	H88
6414.18	3.1	e	d	H91 K95	6792.42	3.1	d	c	H88
6420.77	1.8:	e	d	new	6795.20	4.7	d	d	H88 J94
6425.90	9.3	e	d	H75 H91 K95	6801.41	5.6	d	d	H88 J94
6430.47	2.7	f	e	new	6803.26	2.9	d	d	H88
6439.50	8.7	e	d	H91 K95	6811.27	9.7	d	e	H88
6445.25	13.3	d	d	J94 K95	6820.80	1.3:	d	c	H88
6449.28	5.2	e	d	H75 H91 J94	6823.38	3.1	d	e	H88
				K95	6827.22	9.6	d	c	H88 J94
6455.86	8.6	d	d	new	6834.53	1.3:	e	e	H88
6460.28	6.6	e	d	J94	6837.70	2.9	d	d	H88
6463.41	2.1	e	d	new	6839.05	2.8	e	e	H88
6465.44	1.5:	e	e	new	6841.54	7.8	d	d	H88 J94
6466.65	6.1	e	d	new	6843.69	10.7	d	d	H88 J94
6474.23	3.7	e	d	new	6845.26	1.1:	e	e	H88
6486.75	1.1:	d	d	new	6846.53	2.2	e	d	H88
6489.62	3.6	e	d	new	6852.91:	1.8:	d	d	H88 J94
6492.15	5.5	d	d	J94	6860.13	3.8	e	e	H88 J94
6496.10	2.0	e	d	new	6862.47	1.5:	e	d	H88

4. Results

After averaging we obtained spectra of very high signal-to-noise with enormous number of weak features, which rest wavelengths are estimated using the radial velocities of interstellar sodium lines. The present survey covers spectral range between 5650 and 6865 Å excluding the region of strong telluric O₂ contaminating lines from 6295 to 6350 Å and the region in the vicinity H_α line between 6563 and 6595 Å.

The decision that the feature is interstellar was made after the stellar line test and on the basis of the requirements that it is well seen in our averaged spectra and the spectrum of HD 210839 (the weak interstellar features are generally better seen in “zeta” type spectrum than in “sigma” type spectrum). Our survey does not contain broad DIBs; echelle spectra are not proper tools to search for such features. Thus the newly discovered DIBs are narrow. Such weak features must not be stellar (see the rotational velocities listed in Table 1).

In Table 2 we present all certain DIBs detected in averaged spectra of “sigma” and “zeta” clouds and marked with big asterisks in Fig. 4. The features published in other works are marked without any additional designation (λ 5705.43 for instance) just by segments of straight solid lines.

First column in Table 2 gives the wavelength of the feature measured in the averaged spectrum of “zeta” or “sigma” type (weak features are generally better seen in spectrum of “zeta” cloud). Uncertainties of the wavelengths do not exceed ± 0.1 Å for the features not signed with a colon. Some of the features are extended and their tabulated wavelengths refer to the centre of line. In case of sharp and asymmetric features the measured wavelength originates from the deepest point in the line.

The second column contains equivalent widths (EW) in mÅ for the features measured in the spectrum of HD 210839. Some of the features were blended with stellar and telluric contaminants and they are signed with (bl) as the correct measurement of EW was not possible. In the noisiest regions of the spectra for the very weak features the error in EW can be as large as 50%. Uncertain entries are marked with a colon.

The third and fourth column describe the behaviour of DIBs in the averaged spectra of “sigma” and “zeta” type and the last column contains most important references for every feature.

The data in Table 3 apply to all uncertain features (those which were not clearly seen in all our spectra) and marked with small asterisks in Fig. 4. Most of them are very weak features, reported here for the first time.

5. Discussion

It is quite evident that any rise of the S/N ratio allows to detect new unidentified interstellar features. Apparently

Table 3. List of uncertain DIB’s. Codes as in Table 2

λ_{lab} Å	EW ★ mÅ	In σ cl.	In ζ cl.	references
5657.91		d	d	new
5660.98		d	d	new
5749.06		e	e	new
5800.74		f	e	new
5820.24	1.1:	e	e	new
5919.32	1.7:	e	d	new
5991.63	1.0:	f	e	new
5993.33	1.2:	f	e	new
6000.78		f	d	new
6056.38		e	e	new
6078.18		e	f	new
6111.36		e	e	new
6206.84		f	e	new
6209.90		e	f	new
6218.48	1.2:	e	d	new
...				
6368.72	5.6	e	f	new
6377.09	bl	e	e	new
6433.71	2.0	e	d	new
6436.83	4.9	f	e	new
6468.53	bl	e	f	new
6496.67	0.6:	e	d	new
...				
6691.65	2.5	e	f	new
6744.06	0.5:	e	e	new
6747.80	2.3	e	e	new
6812.80	7.2	e	d	new
6849.66		d	e	new
6855.54	3.7	e	e	new

the absorption spectra of interstellar clouds are very rich – they may contain hundreds of very weak features. They are generally weak and shallow, most of them, observed in averaged spectra (“sigma” and “zeta”) and in the spectrum of HD 210839, are considered as certain. Some of the features listed in Jenniskens & Désert (1994) catalogue are not confirmed in this survey and seen in Table 4. The latter catalogue is based on spectra of only four stars of high reddening. Moreover it involves HD 183143 and HD 21389 – relatively cool stars which spectra may contain many weak stellar lines, unidentified yet. These were possibly listed also as interstellar features. Some of the weak diffuse bands from the Jenniskens and Désert survey differ in wavelength from the features listed in $\Delta\lambda = 0.3$ Å (λ 6284). This may be due to the fact that the survey of Jenniskens and Désert is based on heavily reddened stars towards which the interstellar spectra are formed in many clouds. In such a case it is difficult to decide which of the components of the sodium or calcium lines share the radial velocity with the unidentified features. The wavelengths, listed in Table 2 and Table 3 are corrected to the rest scale using the radial velocities based on Doppler shifts of narrow and symmetrical D_1 and D_2 lines. The line of the interstellar Lithium doublet at 6707.9 Å was seen only

Table 4. Features from Jenniskens & Désert catalogue not listed in our survey (regions 6295 – 6350 Å and 6563 – 6595 Å are excluded)

DIB	Remarks
5747.81	stellar
5853.95	
6045.27	weak and shallow
6177.27	very shallow
6207.83	
6215.71	
6236.58	
6278.89	noisy in our spectra
6280.52	noisy in our spectra
6281.07	noisy in our spectra
6377.87	
6383.04	stellar
6451.60	
6494.17	
6494.91	
6632.10	shallow

in some of our “zeta” type targets with higher reddening. It is, however, quite evident in our average “sigma” and “zeta” objects. It seems to be correlated with narrow DIBs as well as K I and Ca I lines (Krełowski et al. 1998). The fact that our averaging procedure makes this very weak line visible confirms its efficiency in finding weak interstellar features and the fact that the single components of interstellar sodium lines are Doppler-shifted identically to other interstellar lines such as Li I.

Table 4 contains the features from Jenniskens & Désert (1994) catalogue not listed in this survey excluding the region from 6295 to 6350 Å. In echelle spectra broad and shallow features, such as $\lambda 5705$ and $\lambda 5844$ are clearly seen, but generally spectra acquired with the aid of such spectrometers are not proper tools to detect broad spectral features. We cannot thus guarantee that all possible broad and shallow DIBs are listed in our survey. After excluding the region from 6295 to 6350 Å and the region in the vicinity of H_{α} line we found a total of 63 new certain features in the spectral range from 5650 to 6865 Å. Most of them are weak and narrow ones with profiles resembling those observed in the vicinity of $\lambda 5780$ (DIBs at 5766.15, 5772.53 and 5785.11 Å). Their strength ratios are typically different in both kinds of clouds; very weak ones are generally stronger in “zeta” clouds (e.g. new features shortward of $\lambda 6196$). It would be important to divide these weak features into “families” characterized by constant strength ratios to stronger ones. Such “families” are very likely to be spectra of single carriers. Having them listed we should be able to identify the carriers. Precise measurements of rest wavelengths based on Doppler shifts of interstellar sodium lines (perspectively also lines of other interstellar atomic gases) will be helpful while trying to match the spectra acquired in laboratory experiments.

It is to be emphasized that our wavelength estimates are more reliable than those of Jenniskens & Désert (1994) or Ehrenfreund et al. (1997) – both papers based on heavily reddened objects. Such targets are useful while detecting the weak DIBs but not while determining their rest wavelengths. Observing a star through several clouds we do not know which DIB originates in which cloud (they can be either “sigma” or “zeta”). Moreover their profiles can be Doppler-split. This is why we used averaged “sigma” or “zeta” type spectra in this survey.

Acknowledgements. The authors wish to express their gratitude to the staff members of the McDonald Observatory where the spectra have been acquired. The paper was supported financially by the II US–Poland Maria Skłodowska–Curie Joint Fund under the grant MEN/NSF–94–196 and by the Polish State Committee for Scientific Research under the grant 2.PO3D.008.16.

References

- Beals C.S., Blanchet G.H., 1937, PASP 49, 224
 Chlewicki G., de Groot M.S., van der Zwet G.P., Greenburg J.M., Alvarez P.P., Mampaso A., 1987, A&A 173, 131 (**Ch87**)
 Ehrenfreund P., Cami J., Dartois E., Foing B.H., 1997, A&A 318, L28
 Ferlet R., Roueff E., Horani M., Rostas J., 1983, A&A 125, L5 (**F83**)
 Heger M.L., 1922, Lick Obs. Bull. 10, 146
 Herbig G.H., 1975, ApJ 196, 129 (**H75**)
 Herbig G.H., 1988, ApJ 331, 999 (**H88**)
 Herbig G.H., Leka K.D., 1991, ApJ 382, 193 (**H91**)
 Hubeny I., Harmanec P., Stel S., 1995, Bull. Astro. Inst. Czechosl. 37, 370
 Hubeny I., Lanz T., Jeffery C.S., 1995, SYNSPEC – A user’s Guide
 Jenniskens P., Désert F.-X., 1994, A&AS 160, 39 (**J94**)
 Krełowski J., Sneden C., 1993, PASP 105, 1141 (**K93**)
 Krełowski J., Sneden C., Hiltgen D., 1995, Planet. Space Sci. 43, 1195 (**K95**)
 Krełowski J., Schmidt M., Snow T.P., 1997, PASP 109, 1135 (**K97**)
 Krełowski J., Galazutdinov G.A., Musaev F.A., 1998, ApJ 493, 217
 Krełowski J., Walker G.A.H., 1987, ApJ 312, 860
 Krełowski J., Westerlund B.E., 1988, A&A 190, 339
 Kurucz R.L., 1990, Trans. IAU 20b, 169
 Kurucz R.L., 1992, in IAU Symp. 149, Barbuy B. and Renzini A. (eds.), Kluwer, Dordrecht, p. 225
 McCarthy J.K., Sandiford B.A., Boyd D., Booth J., 1993, PASP 105, 881
 Merrill P.W., 1934, PASP 46, 206
 Smith W.H., Snow T.P., Jura M., Cochran W.D., 1981, ApJ 248, 128 (**S81**)
 Piskunov N.E., Kupka F., Ryabchikova T.A., Weiss W.W., Jeffrey C.S., 1995, A&AS 112, 525
 York D.G., 1971, ApJ 166, 65